Analytica Chimica Acta 1088 (2019) 137–143

Contents lists available at ScienceDirect

Analytica Chimica Acta

journal homepage: www.elsevier.com/locate/aca

Cyclodextrin supramolecular inclusion-enhanced pyrene excimer switching for highly selective detection of RNase H

Ye Xie [a], Ningning Wang [b], Yulong Li [a], Ting Deng [a, *], Jishan Li [b], Ke Zhang [a, **], Ruqin Yu [b]

[a] Institute of Applied Chemistry, School of Science, College of Environmental Science and Engineering, Central South University of Forestry and Technology, Changsha, 410004, China
[b] State Key Laboratory of Chemo/Biosensing and Chemometrics, College of Chemistry and Chemical Engineering, Hunan University, Changsha, 410082, China

HIGHLIGHTS

- A novel pyrene excimer switching-based fluorescence method was developed for the highly selective detection of RNase H.
- The sensor exhibited high selectivity both in an ideal solution and in complex biological samples.
- The developed sensor is suitable for evaluating screening potential agents to inhibit RNase H activity.
- The proposed strategy holds the prospect for early diagnosis of diseases associated with abnormal RNase H activity.

GRAPHICAL ABSTRACT

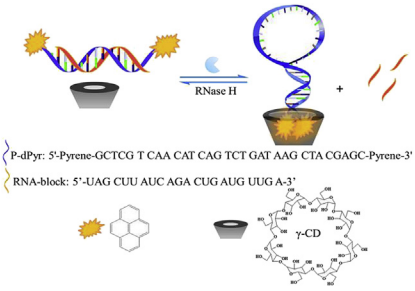

ARTICLE INFO

Article history:
Received 3 June 2019
Received in revised form
13 August 2019
Accepted 25 August 2019
Available online 27 August 2019

Keywords:
RNase H
Pyrene excimer
Inclusion ineraction
Fluorescence
Biosensor

ABSTRACT

Here, we report a novel fluorescence method for the highly selective and sensitive detection of RNase H by combining the use of a dual-pyrene-labeled DNA/RNA duplex with supramolecular inclusion-enhanced fluorescence. Initially, the probe is in the "off" state due to the rigidness of the double-stranded duplex, which separates the two pyrene units. In the presence of RNase H, the RNA strand of the DNA/RNA duplex will be hydrolyzed, and the DNA strand transforms into a hairpin structure, bringing close the two pyrene units which in turn enter the hydrophobic cavity of a γ-cyclodextrin. As a result, the pyrene excimer emission is greatly enhanced, thereby realizing the detection of RNase H activity. Under optimal conditions, RNase H detection can be achieved in the range from 0.08 to 4 U/mL, with a detection limit of 0.02 U/mL.

1. Introduction

Ribonuclease H (RNase H), a family of endogenous ribonucleases discovered in 1969 [1], which can only selectively hydrolyze the phosphodiesters in the RNA strand of a heterologous DNA/RNA heteroduplex [2–4]. Until now, RNase H enzymes have been found to participate not only in DNA replication and repair [5,6], but also

* Corresponding author.
** Corresponding author.
E-mail addresses: muzi_dt@hotmail.com (T. Deng), k.zhang@northeastern.edu (K. Zhang).

https://doi.org/10.1016/j.aca.2019.08.059
0003-2670/

virus reverse transcription [7,8] and antitumor process [9]. Accordingly, abnormal RNase H activity can lead to development of certain diseases. The early diagnosis of a disease is crucial to avoid preventable morbidity and mortality. If the RNase H activity can be detected, then such diseases would be diagnosed in earlier stages and their pathogenic mechanism can be further investigated.

Numerous techniques have been employed to detect the RNase H activity, including gel or capillary electrophoresis [10–13], chromatography methods [14], acidic release of the RNA [15], colorimetry [16,17] and fluorescent methods [18–20]. However, they have obvious drawbacks, such as long time consumptions, toxicity, complexity and inefficiency. Currently, there are several fluorescence methods using nucleic acid probes [21–24], which have been put forward to overcome the drawbacks of those traditional techniques. However, most of these nucleic acid-based fluorescence methods have a similar approach whereby the DNA hairpin loop or stem is designed to have the cleavage site of RNase H, which generates a more or less intense fluorescence signal response in the presence of the another enzyme, like DNase I, an endogenous deoxyribonuclease that can digest single-stranded (ssDNA) or double-stranded (dsDNA). Inadequate specificity will restrict the development of methods and as a result these methods have little chance of being applied for RNase H activity detection in an actual system. Therefore, it is necessary to develop a high specificity and high sensitivity strategy to solve this problem.

Herein, we have developed a proof-of-principle method for a highly sensitive oligonucleotide- and cyclodextrin (CD)-based fluorescent strategy for the selective detection of RNase H (Scheme 1). Pyrene is an organic molecule consisting of four benzene rings that is well-known as fluorophore due to its excellent characteristics, such as high extinction coefficient, quantum yield, and solution stability [25]. With the reduction of the distance between the pyrene molecules acting as fluorescent label, the pyrene in the excited state (monomer) together with the other pyrene in the ground state will produce intramolecular excimer. The pyrene excimer has an emission that is red-shifted by ca. 100 nm compared to the monomer. However, the excimer is unstable and easily disrupted at room temperature [26], and can be affected by environmental conditions [27]. Numerous studies have shown that the truncated corn-shaped cavity of CDs can specifically bind diverse organic molecules to form a robust supramolecular structure [28–32]. There is extensive research about the inclusion interactions of γ-CD and pyrene dimers [33–35], with greatly enhanced fluorescence of the pyrene excimer and increased resistance to environmental factors. Therefore, in this study, we employ the pyrene-CDs inclusion reaction to address the above mentioned problem associated with the pyrene excimers in the context of RNase H detection.

As depicted in Scheme 1, the design involves the labeling of the ssDNA strand by pyrene molecules at both the 3′- and the 5′- termini, whose bases are complementary to an RNA strand. In the presence of RNase H, the RNA sequence of the DNA/RNA duplex is degraded by RNase H. The resulting DNA sequence forms a hairpin structure, bringing the two pyrene units close together. Pyrene excimer can be further stabilized by γ-CD inclusion, which produces stable and readily observable excimer fluorescence. Only RNase H, which hydrolyzes the RNA in the DNA/RNA duplex and release the double pyrene-labeled ssDNA, can lead to the formation of the pyrene excimer. This unique reactivity imparts high specificity to our assay.

2. Materials and methods

2.1. Materials and instruments

The pyrene molecule-labeled ssDNA (P-dPyr: 5′-Pyrene-GCTCG T CAA CAT CAG TCT GAT AAG CTA CGAGC-Pyrene-3′), RNA sequence (RNA-block: 5′-UAG CUU AUC AGA CUG AUG UUG A-3′), and RNase H enzyme were purchased from Takara Biotechnology Co., Ltd. (Dalian, China). All other chemicals were commercially available and used without further purification.

Fluorescence emission spectrum was obtained on a PTI QuantaMaster Fluorescence/Luminescence Spectrometer (Photon Technology International (PTI) Inc., Birmingham, NJ, USA). The fluorescence emission was monitored upon excitation at 344 nm. The slits of excitation and emission were set at 2 nm and 4 nm, respectively. The scan range was set from 365 to 575 nm. The gel image was captured with a Bio-Rad ChemiDoc XRS + Gel imaging system (Bio-Rad Laboratories, Hercules, CA, USA).

2.2. Preparation of the probe system

The mixture of 100 nM P-dPyr and 110 nM RNA-block in a 40 mM Tris–HCl buffer solution (pH 7.8, 80 mM K^+, 16 mM Mg^{2+}, 2 mM DTT) was heated to 90 °C for 5 min and then held at 37 °C for another 2 h, followed by the addition of γ-CD (600 μM). The prepared probe system was stored at 4 °C until used.

2.3. Fluorescence assay using the probe system

RNase H stock solution or other samples were added to 100 μL of the prepared probe system solution and diluted to 200 μL with purified water, and then incubated at 37 °C for 30 min. After the reaction, the resulting reaction solution was subjected to fluorescence measurements as described above.

2.4. Assay of RNase H inhibitor

For the inhibitor assay, various concentrations of the inhibitor (gentamycin sulfate) were first added into 100 μL of the prepared probe system solutions, and then RNase H was added and diluted to 200 μL with purified water (The final concentration of RNase H is 10 U/mL), and then incubated at 37 °C for 30 min. Eventually, the fluorescence emission of the above reaction solutions was monitored as described above.

2.5. Detection of RNase H in serum

For the RNase H activity assay in serum, 2 μL of serum obtained from a mouse and a certain amount of RNase H (the final concentration of RNase H is 10 U/mL) was added into 100 μL of the prepared probe system solutions and diluted to 200 μL with purified water, and then incubated at 37 °C for 30 min. Ultimately, the fluorescence emission of the above reaction solution was monitored as described above.

2.6. Cell culture and RNase H measurement in cell-free extracts

Tumor cells (Hela, Hep G2 and MCF-7) were cultured in DMEM medium. 1×10^6 cells were harvested by trypsin treatment and centrifuged at 1000 rpm for 4 min. Cells were washed 3 times with 5 mL of cold PBS, centrifuged again, and resuspended in 0.5 mL of ice-cold cell lysis buffer and kept on ice for 5 min. Then, extracts were centrifuged at 12,000 rpm for 10 min at 4 °C, and supernatants were collected. The RNase H in cell-free extracts was first detected by using Human RNase H ELISA Kit (Shanghai MLBIO Biotechnology Co., Ltd., Shanghai, China). For the RNase H detection in cell-free extracts using the prepared probe system, 50 μL of the cell-free extracts was added into 100 μL of the prepared probe system solutions and diluted to 200 μL with purified water, and then incubated at 37 °C for 30 min. Eventually, the fluorescence emission of the reaction solution was monitored as described above.

2.7. Gel electrophoresis

The reliability of the proposed sensing method was corroborated by polyacrylamide gel electrophoresis (PAGE) analysis. The samples (P-dPyr, RNA-block, and DNA/RNA duplexes of P-dPyr/RNA-block treated with/without RNase H) were resolved on 20% polyacrylamide gel using 1 × TBE as running buffer, at a constant voltage of 140 V for 120 min. After staining with SYBY Green II (Invitrogen, San Diego, CA, USA), the gel image was captured using a BIO-RAD ChemiDoc XRS + Gel imaging system.

3. Results and discussion

3.1. Validation of the sensing scheme

There are two critically important roles in this sensing method, one is the role of RNase H in biological processes and the other is the hairpin-structured molecular beacon (MB) with dual pyrene labeling. In addition, γ-CD was added to the sensing solution to amplify the fluorescence signal of the pyrene excimer (Fig. S1). As illustrated in Scheme 1, when the whole sensor is in the "off" state, the spatial proximity of pyrene molecules acting as fluorescent label is too long and results in the formation of pyrene monomers but not the pyrene excimer. In the presence of RNase H, the pyrene excimer is formed, due to the short distance between the pyrene pairs acting as fluorescent label after the RNase H hydrolyzes the RNA strand of the DNA/RNA duplex, and thus the sensing ensemble is in the "on" state. The fluorescence signal of the reactant under different conditions was recorded in order to verify the sensing mechanism. The results shown in Fig. 1A reveal that the fluorescence emission of the sensing ensemble at 486 nm is very high due to the presence of the pyrene excimer resulting from the formation of a DNA hairpin structure (black line). However, the fluorescence emission at 486 nm disappeared and a new emission peak appeared at 378 nm upon the addition of the RNA molecule (red line), indicating that the pyrene monomer formed due to the base complementarity between the DNA hairpin and RNA strand. Compared with the results obtained with the P-dPyr/RNA-block duplex (red line), when the DNA/RNA duplexes were treated with RNase H (P-dPyr/RNA-block + RNase H), the fluorescence signal at 486 nm recovered (blue line), indicating that RNase H had hydrolyzed the RNA strand of the DNA/RNA duplexes, and the spatial proximity between the pyrenes molecules acting as fluorescent label decreased, which favors the formation of excimer again, thus resulting in an increase of the fluorescence intensity at 486 nm.

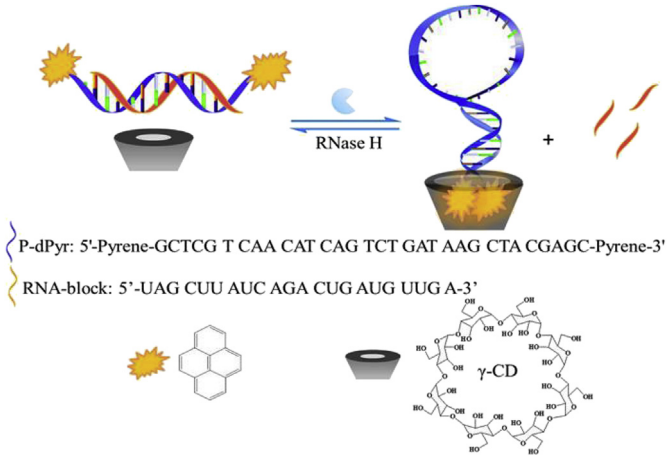

Scheme 1. Schematic illustration of the pyrene excimer switching-based fluorescence sensing ensemble for the RNase H assay.

To further verify the feasibility of the sensor, PAGE analysis was used to detect reaction products. The samples in lanes 1 to 6 (Fig. 1B) were P-dPyr, RNA-block, and DNA/RNA duplexes of P-dPyr/RNA-block treated with/without RNase H, respectively. Comparison of the band pattern in lane 1 and lane 4 or lane 2 and lane 5, clearly reveal that both of them had a band in identical horizontal location, confirming that neither P-dPyr nor RNA-block can be hydrolyzed by RNase H. However, in the presence of RNase H, the DNA/RNA (lane 6) had distinct band pattern compared with lane 3. In addition, lane 6 and lane 1 (P-dPyr) revealed a band pattern with similar location, and both demonstrate that the RNA strand of the DNA/RNA heteroduplex was completely hydrolyzed by RNase H and left the P-dPyr alone in the solution. The consistency between the results of the PAGE analysis and fluorescence spectrometric detection suggests that the sensing scheme for RNase H detection is reliable.

3.2. Optimization of the probe system

The RNA-block should be more excessive than P-dPyr to achieve complete hybridization reaction. However, if the RNA-block is too excessive, it may have an adverse effect on the sensitivity of the sensor system. Therefore, determining the most optimal molar ratio of P-dPyr and RNA-block is highly necessary. Different molar ratios of P-dPyr and RNA-block (1:1, 1:1.1, 1:1.2, 1:1.3) were tested separately to determine the optimal molar ratio. As shown in Fig. 2A, with all of these molar ratios, there was no emission at 486 nm, which indicated not only that the DNA/RNA duplexes had formed, but also that the hybridization reaction of P-dPyr and RNA-block had occurred to completion. Ultimately, the molar ratio of 1:1.1 was selected for use in subsequent assay following the principle that RNA-block should be slightly more excessive than P-dPyr.

Previous studies have shown that the concentration of γ-CD is closely associated with the stability of the stem-loop hairpin structure, and the fluorescence intensity of the excimer can also be quickly enhanced after adding γ-CD. However, an exceedingly high concentration of γ-CD will promote the pyrene/γ-CD inclusion of non-hairpin structures, thus leading to a high excimer fluorescence background. This suggests that it is necessary to choose an optimal concentration of γ-CD in order to make the stem-loop hairpin structure highly stable, and at the same time achieve a high signal-to-background ratio (S/B). As shown in Fig. S2 and Fig. 2B, there was a successive increase in the pyrene excimer signal with an increase of γ-CD concentration after adding RNase H, indicating that more and more pyrene excimer was formed as a result of the pyrene/γ-CD inclusion interaction. At 300 μM γ-CD, the value of the S/B reached to 19, which was 7 times larger than that of the free system without RNase H treatment. Accordingly, 300 μM of γ-CD was chosen for use in subsequent experiments.

To explore the effect of the enzyme reaction time on the performance of the sensor, fluorescence emission was measured at a series of reaction time points, between 0 and 50 min. The results in Fig. 2C showed that the fluorescence increased as a function of reaction time, reaching a plateau after 30 min. Thus, a reaction time of 30 min was used in the follow-up experiments.

3.3. Selectivity and sensitivity

We used this pyrene excimer switching-based sensor to quantify RNase H in a Tris-HCl buffer solution under optimal conditions. As demonstrated above, only with the presence of RNase H in the solution the distance between the two pyrene molecules can be reduced, which then allows the formation of the dimmer structure and the pyrene excimer signal is generated. Thus, the changes in the fluorescence emission intensity at 486 nm can be used to confirm the quantity of RNase H. The relationship between RNase H

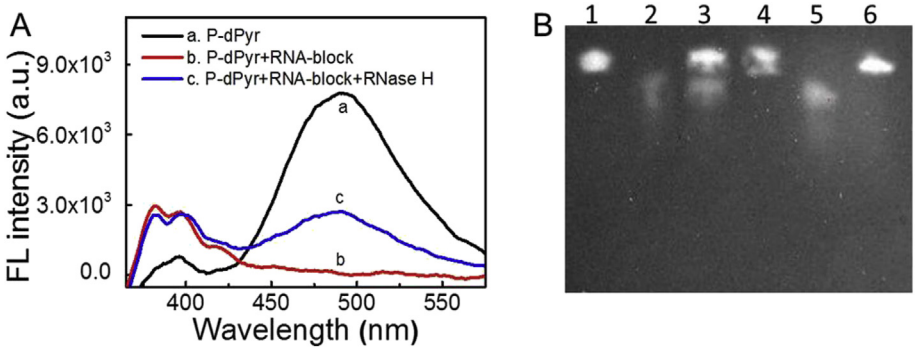

Fig. 1. (A) Fluorescence emission spectra of the P-dPyr solution (50 nM, curve a), P-dPyr/RNA-block duplex solution (50 nM, curve b), and the 50 nM of P-dPyr/RNA-block duplex treated by RNase H (17 U/mL, curve c). (B) polyacrylamide gel electrophoresis (PAGE) analysis: Lane 1, P-dPyr; Lane 2, RNA-block; Lane 3, P-dPyr/RNA-block duplex solution; Lane 4, P-dPyr + RNase H; Lane 5, RNA-block + RNase H; Lane 6, P-dPyr/RNA-block duplex + RNase H. [P-dPyr] = [RNA-block] = 300 nM, [RNase H] = 100 U/mL.

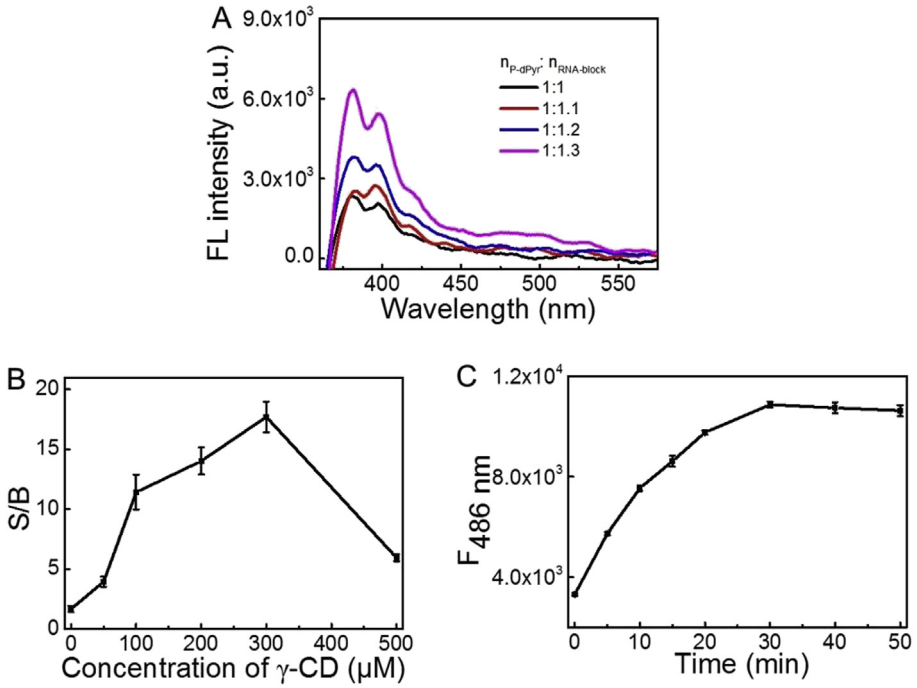

Fig. 2. (A) Fluorescence emission spectra of the mixture solutions of P-dPyr and RNA-block at different molar ratio. (B) Optimization of the concentration of γ-CD for the sensing ensemble (γ-CD: 0, 50, 100, 200, 300, and 500 μM). "S" and "B" are the fluorescence emission intensity at 486 nm for the "P-dPyr/RNA-block duplex + RNase H +γ-CD" solution and the " P-dPyr/RNA-block duplex + γ-CD" solution, respectively. (C) Fluorescence emission intensity at 486 nm of the "P-dPyr/RNA-block duplex + γ-CD + RNase H ″ solution at different incubation time. [P-dPyr] = 50 nM; [RNA-block] = 55 nM; [RNase H] = 17 U/mL.

concentration and the fluorescence intensity of the sensing ensemble depicted in Fig. 3A reveals that the value of the S/B ratio increased gradually with the concentration of RNase H in the range from 0.08 to 4 U/mL ($R^2 = 0.993$). However, it reached a plateau at concentrations higher than 5 U/mL (insert of Fig. 3A), which shows that the reaction between the sensor system and RNase H reached equilibrium at high concentrations of RNase H. The detection limit is 0.02 U/mL, as determined by the 3-delta rule, which is lower than previously published methods (Table 1) [36–40]. We also examined the recovery yield of our method in 2% mouse serum spiked with RNase H. The recoveries ranged from 96% to 116% (Table 2), indicating high reliability. These findings suggest that the proposed sensor functions as intended and may be used to further develop novel and sensitive RNase H activity assays.

We also investigated the capability of the sensor to distinguish RNase H in the presence of other deoxyribonucleases (DNases) or ribonucleases (RNases), including RNase A, DNase I, EXO I, EXO III and S1. The activities of these other enzymes were tested at concentrations 10 times higher than that of RNase H. The data presented in Fig. S3 and Fig. 3B reveal that, other than RNase A, the other nucleases scarcely show any emission at 486 nm, indicating that these enzyme cannot cause the formation of the pyrene excimer, while RNase A showed ~1/5 that of the RNase H activity, which is likely due to the ability of RNase A to specifically hydrolyze RNA cytosine (C) or uracil (U) residues of the DNA/RNA duplex and thus result in the formation of segmental excimer. We also compared the specificity performance of our method vs. other reported methods [21–24]. As shown in Table 3, for our method, in the presence of RNase A, which also cleaves RNA, the signal ratio for RNase H vs. RNase A reached 5, even when RNase A is ten times higher in concentration than RNase H. For other enzymes, the signal ratio can be as high as 20 (the interfering enzyme is always 10x higher in

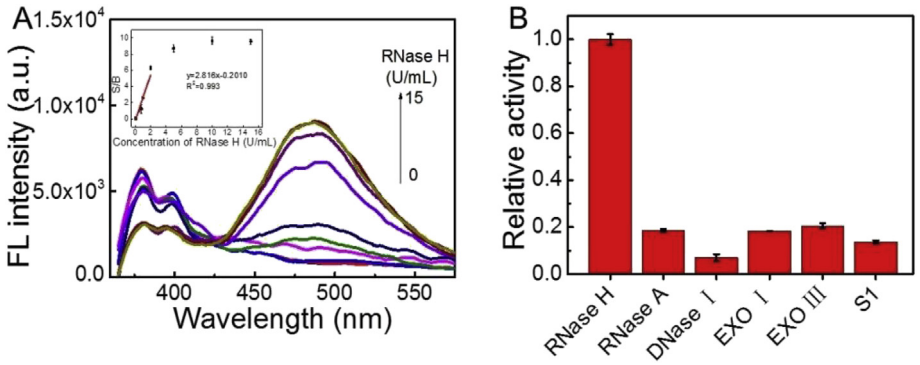

Fig. 3. (A) Fluorescence emission spectra of the sensing ensemble upon varying concentrations of RNase H (0, 0.08, 0.1, 0.5, 1, 2, 5, 10, and 15 U/mL) (Insert: the plot of the fluorescence intensity ratio (S/B) versus RNase H concentration). (B) Bar graph representation of the sensing ensemble solution upon addition of RNase H (3 U/mL) or other enzymes (30 U/mL). Where "B" and "S" are the fluorescence emission intensity at 486 nm of the sensing ensemble before and after addition of the related analyte, respectively. Error bars were calculated from three replicate measurements. [P-dPyr] = 50 nM; [RNA-block] = 55 nM; [γ-CD] = 300 μM.

Table 1
Comparison of the detection limit for RNase H activity using our method vs. other reported methods.

Title	Dtection limit (U/mL)	Linear range (U/mL)	Reference
Real time monitoring of junction ribonuclease activity of RNase H using chimeric molecular beacons	0.5	1–80	[36]
A quadruplex-based, label-free, and real-time fluorescence assay for RNase H activity and inhibition	0.2	0.2–4	[37]
Label-free and nicking enzyme-assisted fluorescence signal amplification for RNase H determination based on a G-quadruplexe/thioflavin T complex	0.03	0.03–1	[38]
A label-free and enzyme-free signal amplification strategy for a sensitive RNase H activity assay	0.037	0–0.7	[39]
Label-free fluorescence assay for rapid detection of RNase H activity based on Tb^{3+}-induced G- quadruplex conjugates	2	0–20	[40]
Cyclodextrin supramolecular inclusion-enhanced pyrene excimer switching for highly selective detection of RNase H	0.02	0.08–4	this work

Table 2
Recovery experiment using 2% mouse serum spiked with RNase H.

Sample	RNase H added (U/mL)	RNase H found (U/mL)	Rcovery (%)
2% mouse serum	0.5	0.58	116
	1	0.96	96
	3	2.92	97

concentration than RNase H). These findings suggest that our approach is highly specific for the RNase H.

3.4. RNase H assay in serum

We also analyzed the activity of different enzymes (RNase H, RNase A, DNase I, EXO I, EXO III and S1) in serum-containing buffer solution in order to further prove that our pyrene excimer-based sensor still has adequate selectivity in a complex biological environment. As shown in Fig. S4A, the pyrene excimer emission with RNase H was still more noticeable than that of the blank samples with other enzymes. At the same time, the activity of RNase A, DNase I, EXO I, EXO III and S1 was still much lower than that of RNase H (Fig. S4B). Together these results demonstrated that our sensor also is also highly specific for RNase H activity detection in biological fluids.

3.5. Detection of RNase H in cell-free extracts

To evaluate the feasibility of the proposed sensing system in complex biological samples, it was applied for RNase H activity analysis in HeLa, HepG2 and MCF-7 cell-free extracts. As shown in Fig. 4A, the fluorescence emission at 486 nm can be attributed to the increased formation of pyrene excimers after adding the cell-free extracts from these three cell lines, indicating that HeLa, HepG2 and MCF-7 cell-free extracts all contain RNase H. Moreover, we also can find that the highest RNase H activity in the cell-free extract was in that from MCF-7 cells (5.925 U/mL), followed by HepG2 (4.606 U/mL), and the lowest was that in HeLa (3.975 U/mL). The results shown in Fig. 4B also reveal that the actual values of RNase H detected by enzyme linked immunosorbent assay (ELISA) analysis (Fig. S5 and Table S1: 42.95 ± 10.89 IU/L for HeLa, 47.45 ± 7.33 IU/L for HepG2, and 58.55 ± 4.44 IU/L for MCF-7) and

Table 3
Comparison of specificity performance for the detection of RNase H activity using our method vs. other reported methods.

Cleavage site	[RNase H]/[other enzymes]	Signal ratio of RNase H/other enzyme	Reference
The loop of DNA hairpin	1	~4–11	[21]
The stem of DNA hairpin	1	~4–6	[22]
The stem of DNA hairpin	1	~7–8	[23]
The stem of DNA hairpin	0.6	~6–8	[24]
The RNA strand of DNA/RNA duplex	0.1	~5–20	this work

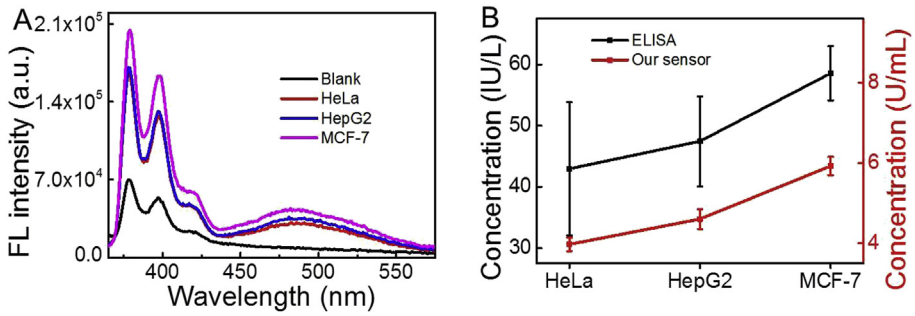

Fig. 4. (A) Fluorescence emission spectra of the sensing ensemble upon addition of different cell-free extracts (HeLa, HepG2 and MCF-7). (B) The concentration of RNase H in different cell-free extracts (HeLa, HepG2 and MCF-7) detected by our method (red) and ELISA (black). The sensing result was obtained from "A" and the equation of $y = 2.811x+0.7989$, and the ELISA result was was obtained from Fig. S5 and Table S1. [P-dPyr] = 50 nM; [RNA-block] = 55 nM; [γ-CD] = 300 μM. (For interpretation of the references to color in this figure legend, the reader is referred to the Web version of this article.)

our sensor in these three cell lines were different, which was due to the fact that ELISA measured the protein contents of RNase H and our assay measured the activity value of RNase H. Nevertheless, the detection of the RNase H activity detection by our sensor showed a satisfactory correlation with that by ELISA. These results suggest that we developed a method to reliably measure RNase H activity in complex biological samples, such as cell-free extracts.

3.6. Effects of gentamycin sulfate on the RNase H activity assay

RNase H is associated with several reverse transcriptase enzymes, which paves the way for the development of a novel and attractive antiviral therapeutics [41]. Accordingly, we chose gentamycin sulfate as an RNase H model inhibitor for assessing the capability of our sensor to screen for RNase H inhibitors [42]. As shown in Fig. 5, the relative activity of RNase H decreased gradually with increasing gentamycin sulfate concentration, demonstrating its inhibitory effect against RNase H activity. The IC_{50} value (the inhibitor concentration required to reduce the enzyme activity by 50%) of gentamycin sulfate obtained from the lots of maximum fluorescence intensity versus the concentration of gentamycin sulfate, is 70 ± 6 μM, which shows a great agreement with previous report [36]. Thus, the results clearly demonstrated that the developed sensor is quite suitable for evaluating antibiotic inhibitors and screening potential agents to inhibit RNase H activity.

4. Conclusions

In summary, we have developed a novel fluorescence method for the highly selective and sensitive detection of RNase H by combining a DNA/RNA duplex with a cyclodextrin supramolecular inclusion-enhanced pyrene excimer switching. Due to a smart sensing mechanism, this method exhibited high selectivity both in an ideal solution and in complex biological samples. Furthermore, the use of gentamycin sulfate as an RNase H model inhibitor allowed us to verify the capability of our method to screen for RNase H antibiotics inhibitors. Of note, the emission wavelength of pyrene excimer is in the range of 365–575 nm, which is compounded by biological autofluorescence. However, the lifetime of the pyrene excimer is about 60–100 ns, while that for most bio-autofluorescence is less than 10 ns, which can in principle be used to reduce background signals. These results suggest that the proposed strategy not only provides a highly specific platform to detect RNase H activity, but also can be expanded into actual biological systems, especially when time-resolved fluorescence technique is employed. Thus, our method is a promising new technique for early diagnosis of diseases associated with abnormal RNase H activity.

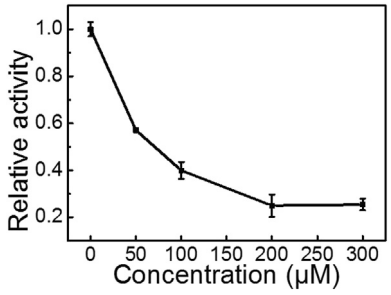

Fig. 5. Effect of gentamycin sulfate on the RNase H activity assay. [P-dPyr] = 50 nM, [RNA-block] = 55 nM, [γ-CD] = 300 μM, [RNase H] = 10 U/mL.

Declaration of competing interest

The authors declare that they have no known competing financial interests or personal relationships that could have appeared to influence the work reported in this paper.

Acknowledgements

This work was supported by the National Natural Science Foundation of China (21775035), Hunan Provincial Natural Science Foundation (2016JJ1005) and Outstanding youth project of Hunan Provincial Department of Education (18B182).

Appendix A. Supplementary data

Supplementary data to this article can be found online at https://doi.org/10.1016/j.aca.2019.08.059.

References

[1] H. Stein, P. Hausen, Enzyme from calf thymus degrading the RNA moiety of DNA-RNA hybrids: effect on DNA-dependent RNA polymerase, Science 166 (1969) 393–395.
[2] S.M. Cerritelli, R.J. Crouch, Ribonuclease H: the enzymes in eukaryotes, FEBS J. 276 (2009) 1494–1505.
[3] T. Tadokoro, S. Kanaya, Ribonuclease H: molecular diversities, substrate binding domains, and catalytic mechanism of the prokaryotic enzymes, FEBS J. 276 (2009) 1482–1493.
[4] S. Kanaya, M. Ikehara, Functions and structures of ribonuclease H enzymes, Subcell. Biochem. 24 (1995) 377–422.
[5] D. Bubeck, M.A. Reijns, S.C. Graham, K.R. Astell, E.Y. Jones, A.P. Jackson, PCNA directs type 2 RNase H activity on DNA replication and repair substrates, Nucleic Acids Res. 39 (2011) 3652–3666.
[6] F. Lazzaro, D. Novarina, F. Amara, D.L. Watt, J.E. Stone, V. Costanzo, et al., RNase H and postreplication repair protect cells from ribonucleotides incorporated

in DNA, Mol. Cell 45 (2012) 99–110.
[7] K.A. Delviks-Frankenberry, G.N. Nikolenko, V.K. Pathak, The "connection" between HIV drug resistance and RNase H, Viruses 2 (2010) 1476–1503.
[8] G.R. Nakayama, P. Bingham, D. Tan, K.A. Maegley, A fluorescence polarization assay for screening inhibitors against the ribonuclease H activity of HIV-1 reverse transcriptase, Anal. Biochem. 351 (2006) 260–265.
[9] W.F. Lima, S.T. Crooke, Cleavage of single strand RNA adjacent to RNA-DNA duplex regions by Escherichia coli RNase H1, J. Biol. Chem. 272 (1997) 27513–27516.
[10] K.C. Chan, S.R. Budihas, S.F.J. Le Grice, M.A. Parniak, R.J. Crouch, S.A. Gaidamakov, et al., A capillary electrophoretic assay for ribonuclease H activity, Anal. Biochem. 331 (2004) 296–302.
[11] M. Haruki, Y. Tsunaka, M. Morikawa, S. Kanaya, Cleavage of a DNA–R-NA–DNA/DNA chimeric substrate containing a single ribonucleotide at the DNA–RNA junction with prokaryotic RNases HII, FEBS (Fed. Eur. Biochem. Soc.) Lett. 531 (2002) 204–208.
[12] H. Huang, J. Liao, S.N. Cohen, Poly(A)- and poly(U)-specific RNA 3′ tail shortening by E. coli ribonuclease E, Nature 391 (1998) 99–102.
[13] N. Ohtani, M. Tomita, M. Itaya, Junction ribonuclease: a ribonuclease HII orthologue from Thermus thermophilus HB8 prefers the RNA–DNA junction to the RNA/DNA heteroduplex, Biochem. J. 412 (2008) 517–526.
[14] U. Arnold, R. Ulbrich-Hofmann, Natural and engineered ribonucleases as potential cancer therapeutics, Biotechnol. Lett. 28 (2006) 1615–1622.
[15] D.S. Choi, J.H. Kim, U.S. Shin, R.R. Deshmukh, C.E. Song, Thermodynamically- and kinetically-controlled Friedel-Crafts alkenylation of arenes with alkynes using an acidic fluoroantimonate(v) ionic liquid as catalyst, Chem. Commun. (2007) 3482–3484.
[16] X. Xie, W. Xu, T. Li, X. Liu, Colorimetric detection of HIV-1 ribonuclease H activity by gold nanoparticles, Small 7 (2011) 1393–1396.
[17] C. Vasti, D.A. Bedoya, R. Rojas, C.E. Giacomelli, Effect of the protein corona on the colloidal stability and reactivity of LDH-based nanocarriers, J. Mater. Chem. B 4 (2016) 2008–2016.
[18] J.H. Kim, R.A. Estabrook, G. Braun, B.R. Lee, N.O. Reich, Specific and sensitive detection of nucleic acids and RNases using gold nanoparticle–RNA–fluorescent dye conjugates, Chem. Commun. (2007) 4342–4344.
[19] Y. Zhang, Z. Li, Y. Cheng, X. Lv, Colorimetric detection of microRNA and RNase H activity in homogeneous solution with cationic polythiophene derivative, Chem. Commun. (2009) 3172–3174.
[20] J.H. Kim, R.A. Estabrook, G. Braun, B.R. Lee, N.O. Reich, Specific and sensitive detection of nucleic acids and RNases using gold nanoparticle-RNA-fluorescent dye conjugates, Chem. Commun. (42) (2007) 4342–4344.
[21] C. Zhao, J. Fan, L. Peng, L. Zhao, C. Tong, W. Wang, et al., An end-point method based on graphene oxide for RNase H analysis and inhibitors screening, Biosens. Bioelectron. 90 (2017) 103–109.
[22] K. Zhang, Q. Yang, W. Huang, K. Wang, X. Zhu, M. Xie, Detection of HIV-1 ribonuclease H activity in single-cell by using RNA mimics green fluorescent protein based biosensor, Sens. Actuators B Chem. 281 (2019) 439–444.
[23] L. Wang, H. Zhou, B. Liu, C. Zhao, J. Fan, W. Wang, et al., Fluorescence assay for ribonuclease H based on nonlabeled substrate and DNAzyme assisted cascade amplification, Anal. Chem. 89 (2017) 11014–11020.
[24] Y. Jung, C.Y. Lee, K.S. Park, H.G. Park, Target-activated DNA polymerase activity for sensitive RNase H activity assay, Biotechnol. J. 14 (2019) 1800645.
[25] K.J. Oh, K.J. Cash, K.W. Plaxco, Excimer-based peptide Beacons: a convenient experimental approach for monitoring Polypeptide–Protein and Polypeptide–Oligonucleotide interactions, J. Am. Chem. Soc. 128 (2006) 14018–14019.
[26] J.B. Birks, Excimers, Rep. Prog. Phys. 38 (1975) 904–974.
[27] X. Gao, T. Deng, J. Li, R. Yang, G. Shen, R. Yu, New probe design strategy by cooperation of metal/DNA-ligation and supermolecule inclusion interaction: application to detection of mercury ions(II), Analyst 138 (2013) 2755–2760.
[28] T. Ihara, A. Uemura, A. Futamura, M. Shimizu, N. Baba, S. Nishizawa, et al., Cooperative DNA probing using a β-cyclodextrin–DNA conjugate and a nucleobase-specific fluorescent ligand, J. Am. Chem. Soc. 131 (2009) 1386–1387.
[29] Y. Liu, L. Yu, Y. Chen, Y.L. Zhao, H. Yang, Construction and DNA condensation of cyclodextrin-based polypseudorotaxanes with anthryl grafts, J. Am. Chem. Soc. 129 (2007) 10656–10657.
[30] J. Szejtli, Introduction and general overview of cyclodextrin chemistry, Chem. Rev. 98 (1998) 1743–1754.
[31] H. Yan, L. He, W. Zhao, J. Li, Y. Xiao, R. Yang, et al., Poly β-cyclodextrin/TPdye nanomicelle-based two-photon nanoprobe for caspase-3 activation imaging in live cells and tissues, Anal. Chem. 86 (2014) 11440–11450.
[32] H. Yan, L. He, C. Ma, J. Li, J. Yang, R. Yang, et al., Poly β-cyclodextrin inclusion-induced formation of two-photon fluorescent nanomicelles for biomedical imaging, Chem. Commun. 50 (2014) 8398–8401.
[33] A.S.M. Dyck, U. Kisiel, C. Bohne, Dynamics for the assembly of pyrene–γ-cyclodextrin Host–Guest complexes, J. Phys. Chem. B 107 (2003) 11652–11659.
[34] T. Yorozu, M. Hoshino, M. Imamura, Fluorescence studies of pyrene inclusion complexes with .alpha.-, .beta.-, and .gamma.-cyclodextrins in aqueous solutions. Evidence for formation of pyrene dimer in .gamma.-cyclodextrin cavity, J. Phys. Chem. 86 (1982) 4426–4429.
[35] Q. Zhang, T. Deng, J. Li, W. Xu, G. Shen, R. Yu, Cyclodextrin supramolecular inclusion-enhanced pyrene excimer switching for time-resolved fluorescence detection of biothiols in serum, Biosens. Bioelectron. 68 (2015) 253–258.
[36] B. Liu, D. Xiang, Y. Long, C. Tong, Real time monitoring of junction ribonuclease activity of RNase H using chimeric molecular beacons, Analyst 138 (2013) 3238–3245.
[37] D. Hu, F. Pu, Z. Huang, J. Ren, X. Qu, A quadruplex-based, label-free, and real-time fluorescence assay for RNase H activity and inhibition, Chem. Eur J. 16 (2010) 2605–2610.
[38] K. Wu, C. Ma, Z. Deng, N. Fang, Z. Tang, X. Zhu, et al., Label-free and nicking enzyme-assisted fluorescence signal amplification for RNase H determination based on a G-quadruplexe/thioflavin T complex, Talanta 182 (2018) 142–147.
[39] C.Y. Lee, H. Jang, K.S. Park, H.G. Park, A label-free and enzyme-free signal amplification strategy for a sensitive RNase H activity assay, Nanoscale 9 (2017) 16149–16153.
[40] K. Wu, C. Ma, H. Liu, H. He, W. Zeng, K. Wang, Label-free fluorescence assay for rapid detection of RNase H activity based on Tb3+-induced G-quadruplex conjugates, Anal. Methods 9 (2017) 3055–3060.
[41] A. Derosier, H. Overton, J.A. Martin, J.Q. Hang, K.E.B. Parkes, K. Klumpp, et al., Two-metal ion mechanism of RNA cleavage by HIV RNase H and mechanism-based design of selective HIV RNase H inhibitors, Nucleic Acids Res. 31 (2003) 6852–6859.
[42] N. Wang, L. Song, H. Xing, K. Zhang, R. Yang, J. Li, A spherical nucleic acid-based two-photon nanoprobe for RNase H activity assay in living cells and tissues, Nanoscale 11 (2019) 8133–8137.